Supporting Information

Carbon supported PdNi alloy nanoparticles on SiO_2 nanocages with enhanced catalytic performance

Min Zhang*[a], Yang Ling,[a] Libin Liu [b*], Jingli Xu[a], Jiaxing Li[c], Qunling Fang[d*].

[a.] *College of Chemistry and Chemical Engineering, Shanghai University of Engineering Science, Shanghai 201620, PR China. E-mail:* zhangmin@sues.edu.cn.

[b.] *School of Chemistry and Pharmaceutical Engineering, Qilu University of Technology (Shandong Academy of Sciences), Jinan 250353, China. E-mail: lbliu@qlu.edu.cn*

[c.] *Institute of Plasma Physics, Chinese Academy of Sciences, P.O. Box 1126, 230031 Hefei, PR China*

[d.] *School of Food and Biological Engineering, Key Laboratory of Metabolism and Regulation for Major Diseases of Anhui Higher Education Institutes, Hefei University of Technology, Hefei, 230009, PR China E-mail:fql.good@hfut.edu.cn*

Synthesis of SiO_2@C-AgNi and SiO_2@C-AuNi

In a typical synthesis, 0.02 g of as-prepared SiO_2@C-Ni was initially dispersed in 10 mL of ethanol to form a uniform suspension via ultrasonication. Then, 35 mL of aqueous solution containing 3 mg of $AgNO_3$ was added. Then, this reaction solution was transferred into a 100 mL three-necked flask with mechanical stirring and heated at 65 °C for 3 h. After cooling, the product was collected by centrifugation and washed with water and ethanol for several times before drying at 50 °C overnight. The preparation of SiO_2@C-AuNi was basically the same as that of SiO_2@C-AgNi except the $AgNO_3$ was replaced with $HAuCl_4$.

Catalytic degradation of methylene blue

The reduction of methylene blue (MB) was carried out in a quartz cuvette at room temperature. 0.2 mg of the as-prepared catalysts was added into a solution with MB (10 mL, 20mg /L). Then, 10 mg of $NaBH_4$ was added. The reaction progress was monitored by using a UV-vis absorption spectrometer (UV-2450, Shimadzu) in the scanning range of 450-800 nm at room temperature.

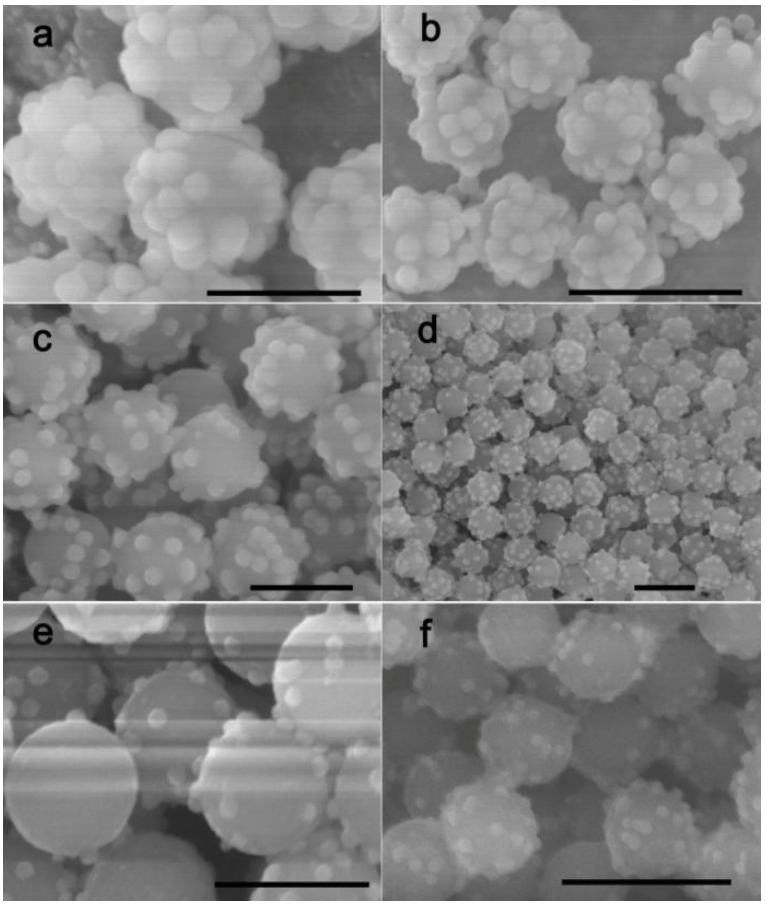

Fig. S1 SEM image of CPS@SiO_2 with the amount of CPS 25 mg (a, b), 100 mg (c, d), 150 mg (e, f). Scale bars: 300 nm in (a, c, e), and 500 nm in (b, d, f).

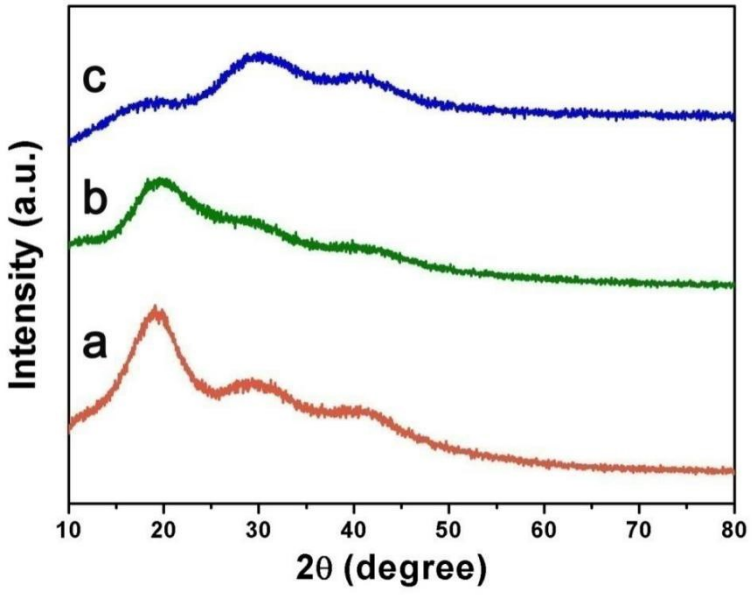

Fig. S2 XRD diffraction patterns of CPS (a); CPS@SiO_2 (b) and CPS@SiO_2@RF-Ni^{2+} (c).

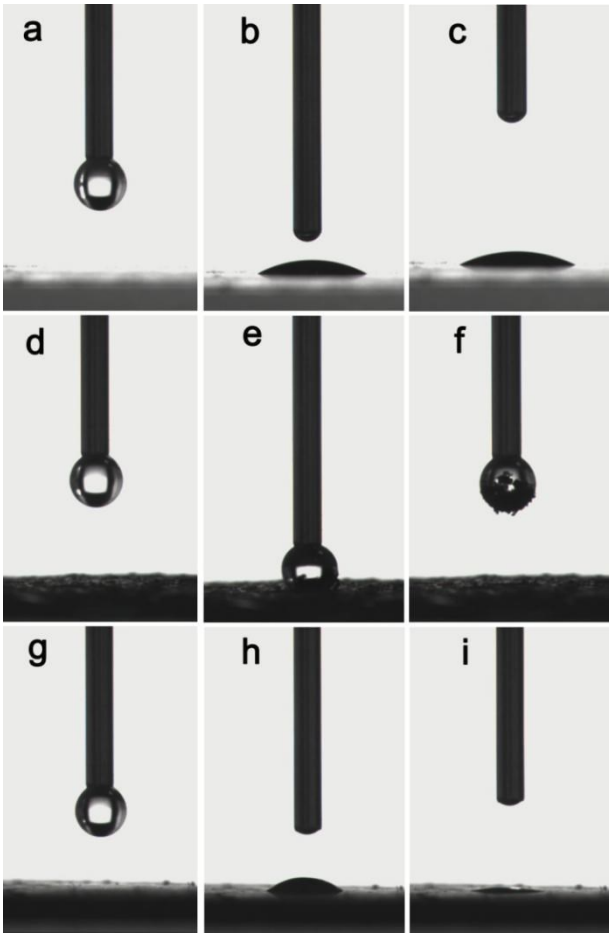

Fig. S3 Photographs of water droplets on surfaces of CPS@SiO_2@RF-Ni^{2+} (a, b, c), SiO_2@C-Ni (d, e, f) and SiO_2@C-PdNi (g, h, i).

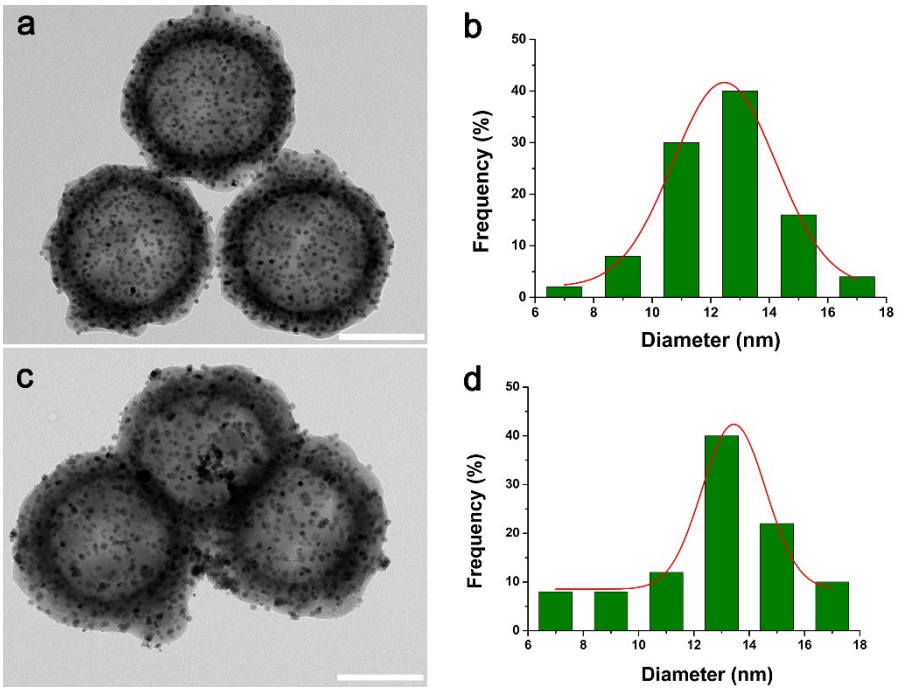

Fig. S4 (a, c) TEM images of SiO_2@C-Ni and SiO_2@C-PdNi respectively; (b, d) the distribution curve of Ni NPs diameter (b, SiO_2@C-Ni and d, SiO_2@C-PdNi); Scale bars: 200 nm in (a, c).

Table S1 the average diameter of Ni NPs

Sample	The average diameter of Ni NPs (nm)
SiO_2@C-Ni	12.34
SiO_2@C-PdNi	12.83

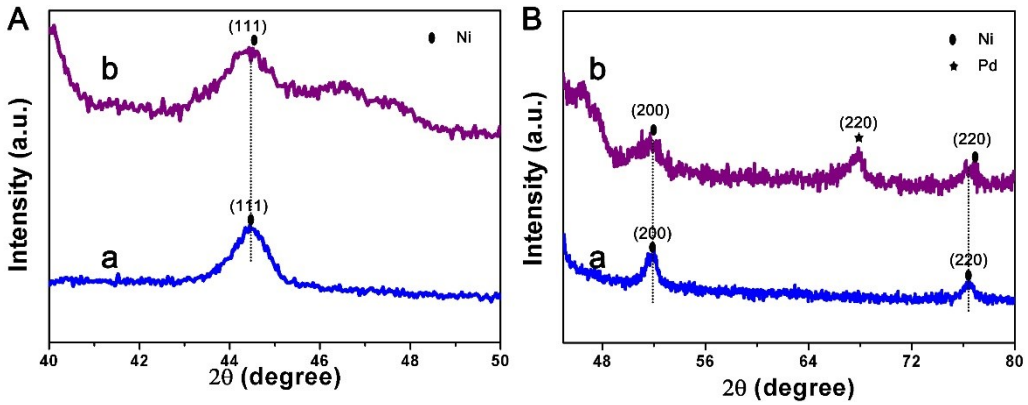

Fig. S5 Enlarged XRD diffraction patterns of SiO_2@C-Ni(a) and SiO_2@C-PdNi (b).

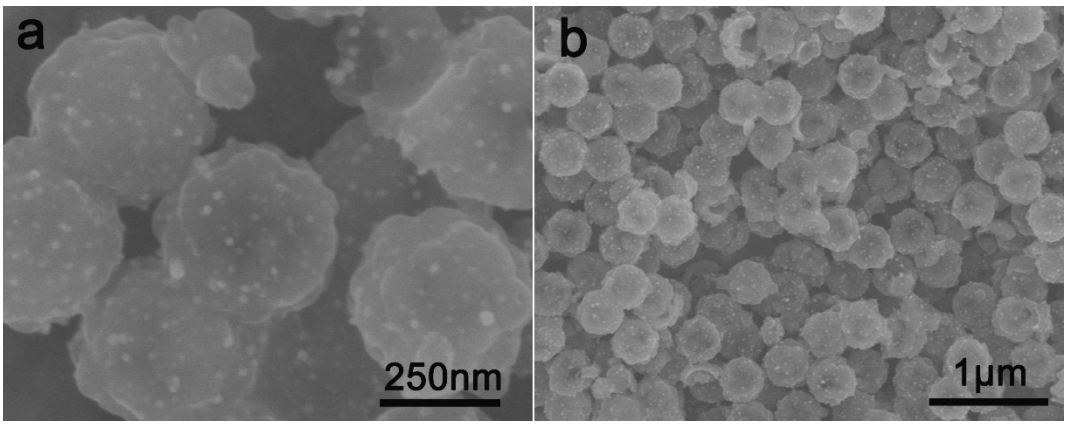

Fig. S6 SEM images of the SiO_2@C-PdNi (1mg).

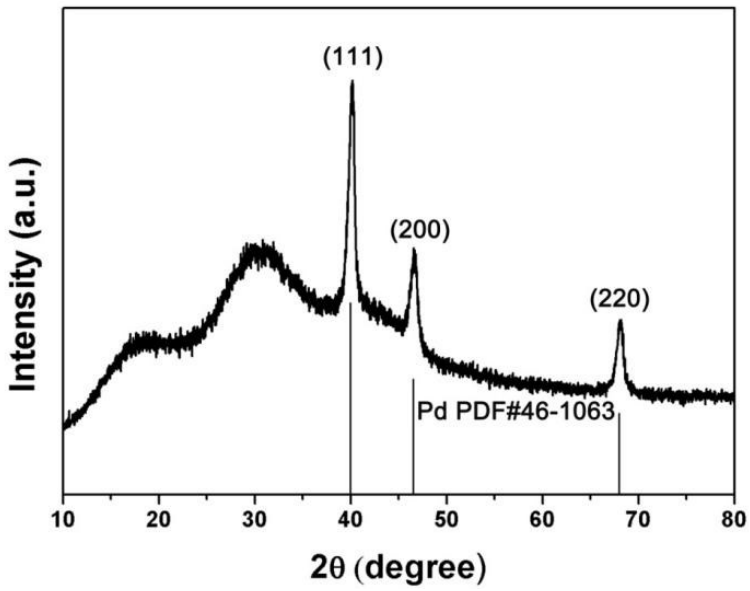

Fig. S7 XRD diffraction patterns of SiO_2@C-PdNi(10mg).

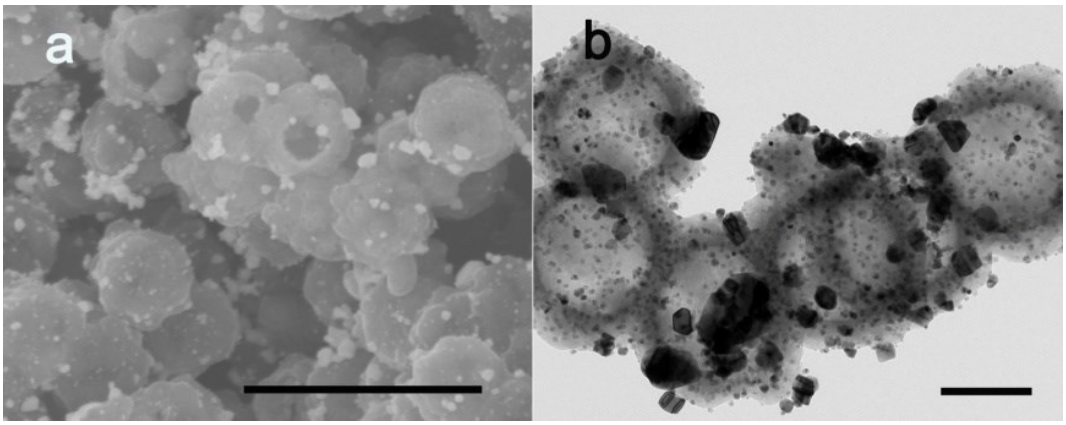

Fig. S8 SEM and TEM images of SiO_2@C-PdNi (10mg). Scale bars: 1 μm in (a), and 200 nm in (b).

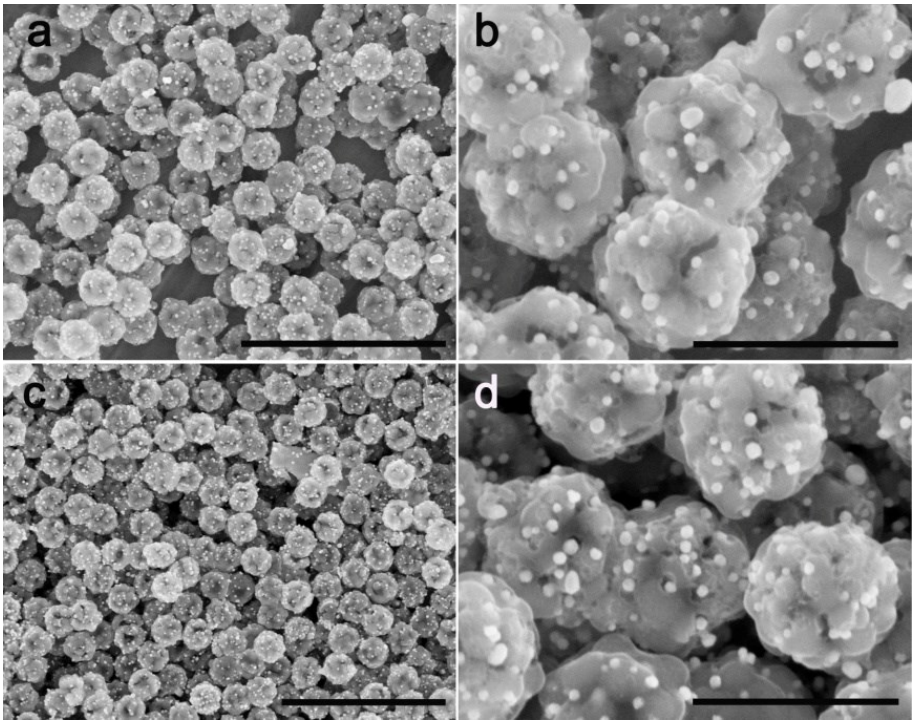

Fig. S9 SEM images of SiO_2@C-AgNi (a, b) and SiO_2@C-AuNi (c, d). Scale bars: 2 μm in (a, c), and 500 nm in (b, d).

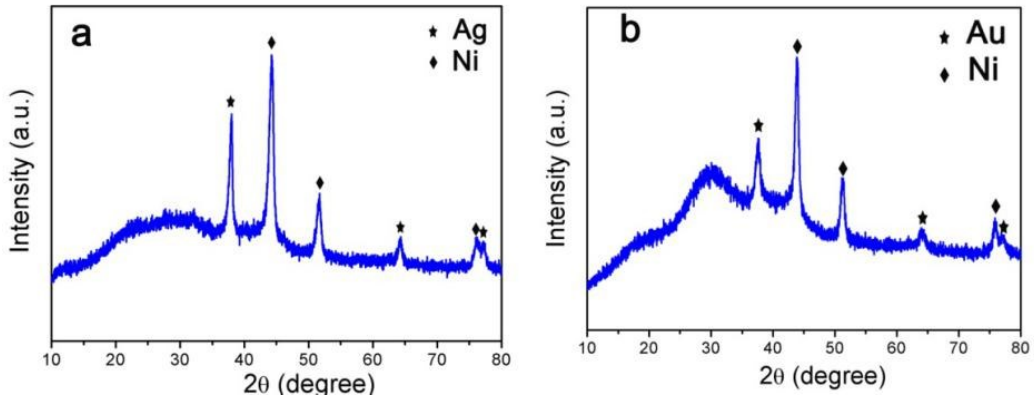

Fig. S10 XRD diffraction patterns of SiO_2@C-AgNi(a), SiO_2@C-AuNi(b). (Ag: JCPDS no. 04-0783, Au: JCPDS no. 04-0784).

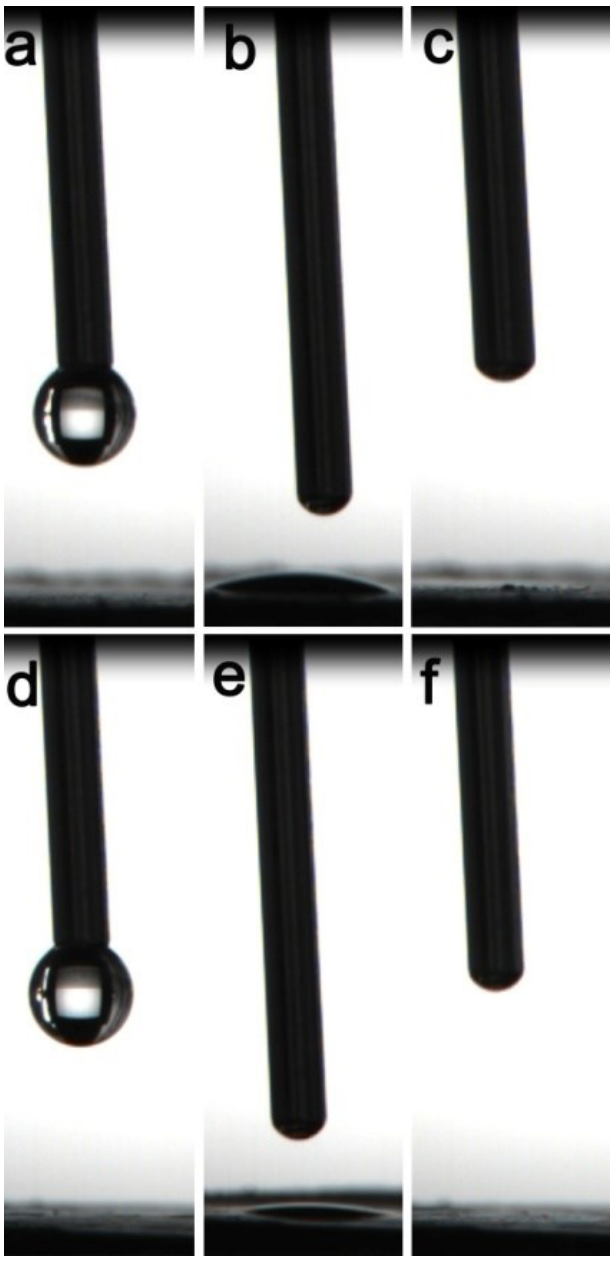

Fig. S11 Photographs of water droplets on surfaces of SiO_2@C-AgNi (a, b, c), and SiO_2@C-AuNi (d, e, f).

Table S2 ICP data of SiO_2@C-Ni and SiO_2@C-PdNi

Catalyst	Ni(μg/mg)	Pd (μg/mg)
SiO_2@C-Ni	143.6	-
SiO_2@C-PdNi	49.31	43.97

Table S3 A full comparison of the activity parameter κ of SiO_2@C-Ni and SiO_2@C-PdNi hollow hybrid composites with other noble metal and no-noble catalysts

Samples	K ($\times10^{-3}s^{-1}$)	κ ($\times10^{-3}mg^{-1}s^{-1}$)	References
SiO_2@C-Ni	1.79	62.33	This work
SiO_2@C-PdNi	4.56	244.42	This work
Ag/Cu	6.70	74	46
Ag/Si	38.41	142.46	47
Ni/C	6.26	20.9	48
Ag@Pd-Graphene	8.67	86.7	49
AuPd	5.2	74	50
Cu_2O-Cu-CuO	10.4	20.7	51
PtPdBi	4.3	287	52
Fe@Au-ATPGO	1.4	400	53

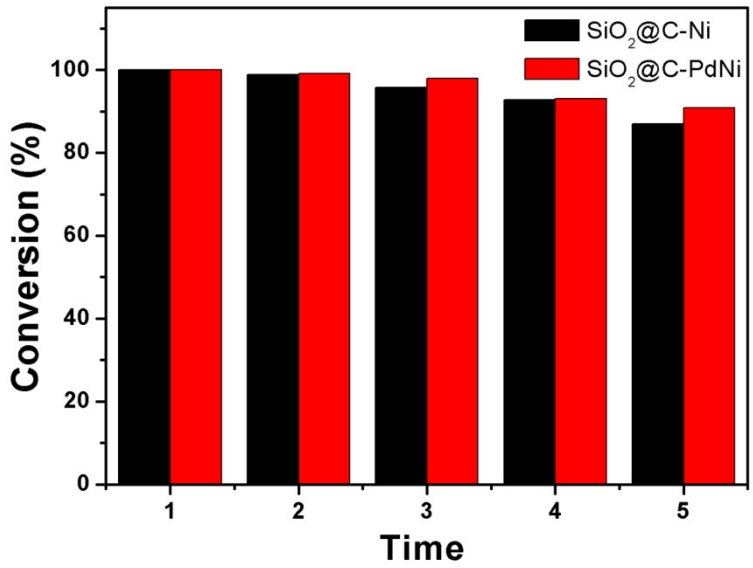

Fig. S12 cycle test of the SiO_2@C-Ni and SiO_2@C-PdNi.

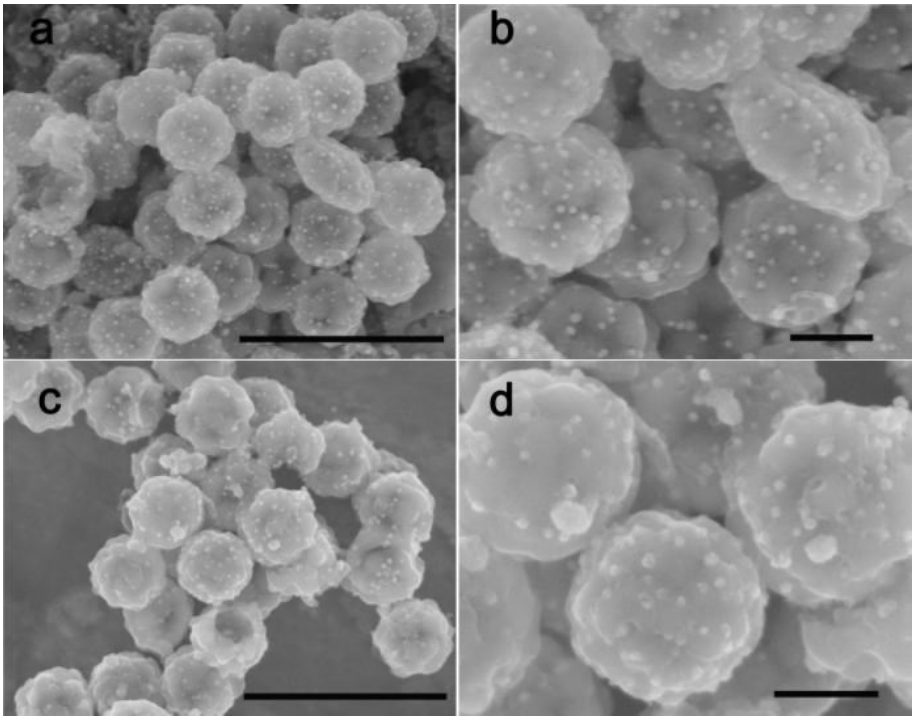

Fig. S13 SEM images of SiO_2@C-Ni (a, b) and SiO_2@C-PdNi (c, d) after five catalytic. Scale bars: 1 μm in (a, c), and 200 nm in (b, d).

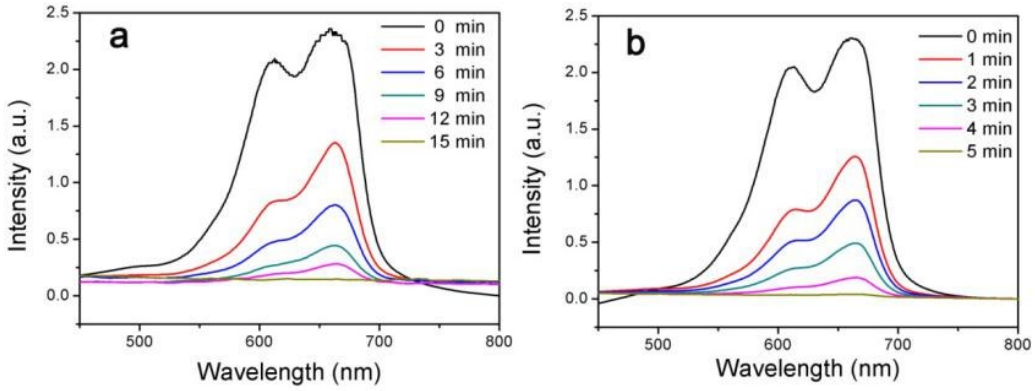

Fig. S14 UV-Vis absorption spectra of MB during the reduction catalyzed by SiO_2@C-Ni composite (a) and SiO_2@C-PdNi (b).

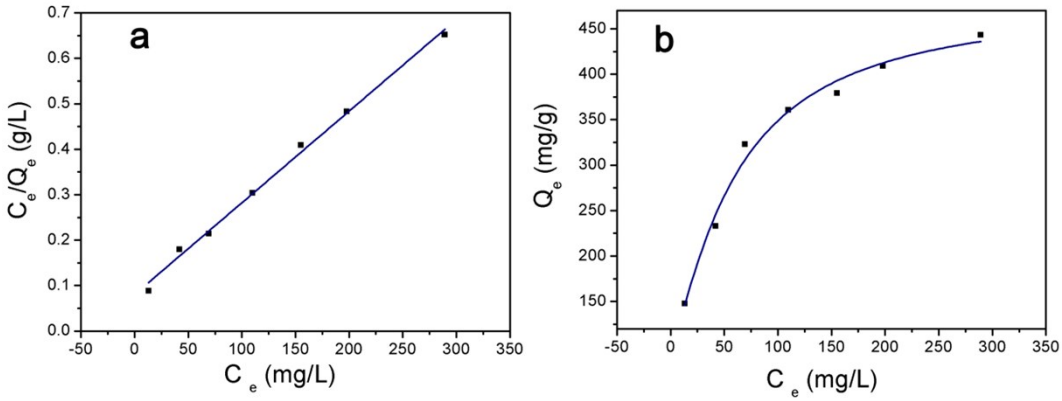

Fig. S15 Linear fitting of adsorption isotherms plots Langmuir model (a), and adsorption isotherm of BHb on SiO_2@C-Ni the solution containing 20 mM phosphate at pH 7.0-8.0 (b).

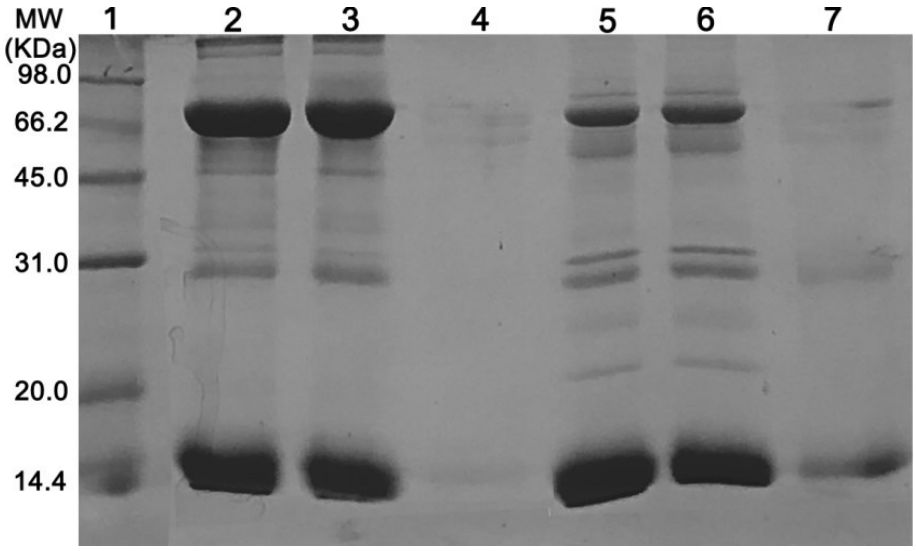

Fig. S16 SDS-PAGE analysis of adsorption by SiO_2@C-Ni composites from solution. Lane 1, marker; lane 2, 1 mg·mL^{-1} of BHb and BSA binary solution; lane 3, the supernant BHb and BSA solution after treated with SiO_2@C-Ni composites; lane 4, the eluted BHb and BSA mixture by 0.2 g·mL^{-1} 2-methylimidazole solution; lane 5, diluted 100-fold human whole blood; lane 6, supernant human whole blood solution after treated by SiO_2@C-Ni composites; lane 7, the eluted 100-fold human whole blood by 0.2 g·mL^{-1} 2-methylimidazole solution.

---

46. Y. Sun, F. Zhang, L. Xu, Z. Yin and X. Song, Roughness-controlled copper nanowires and Cu nanowires-Ag heterostructures: synthesis and their enhanced catalysis, *Journal of Materials Chemistry A*, 2014, **2**, 18583-18592.

47. Z. Zhang, C. Shao, Y. Sun, J. Mu, M. Zhang, P. Zhang, Z. Guo, P. Liang, C. Wang and Y. Liu, Tubular nanocomposite catalysts based on size-controlled and highly dispersed silver nanoparticles assembled on electrospun silica nanotubes for catalytic reduction of 4-nitrophenol, *Journal of Materials Chemistry*, 2011, **22**, 1387-1395.

48. Y. Yang, Y. Ren, C. Sun and S. Hao, Facile route fabrication of nickel based mesoporous carbons with high catalytic performance towards 4-nitrophenol reduction, *Green Chemistry*, 2014, **16**, 2273.

49. C. H. Liu, X. Q. Chen, Y. F. Hu, T. K. Sham, Q. J. Sun, J. B. Chang, X. Gao, X. H. Sun and S. D. Wang, One-pot environmentally friendly approach toward highly catalytically active bimetal-nanoparticle-graphene hybrids, *Applied Materials & Interfaces*, 2013, **5**, 5072-5079.

50. J. Zhang, C. Hou, H. Huang, L. Zhang, Z. Jiang, G. Chen, Y. Jia, Q. Kuang, Z. Xie and L. Zheng, Surfactant-concentration-dependent shape evolution of Au-Pd alloy nanocrystals from rhombic dodecahedron to trisoctahedron and hexoctahedron, *Small*, 2013, **9**, 538-544.

51. A. K. Sasmal, S. Dutta and T. Pal, A ternary Cu_2O-Cu-CuO nanocomposite: a catalyst with intriguing activity, *Dalton transactions*, 2016, **45**, 3139-3150.

52. Y. Y. Shen, Y. Sun, L. N. Zhou, Y. J. Li and E. Yeung, Synthesis of ultrathin PtPdBi nanowire and its enhanced catalytic activity towards p-nitrophenol reduction, *Journal of Materials Chemistry A*, 2014, **2**, 2977-2984.

53. V. K. Gupta, N. Atar, M. L. Yola, Ü. Z and L. Uzun, A novel magnetic Fe@Au core-shell nanoparticles anchored graphene oxide recyclable nanocatalyst for the reduction of nitrophenol compounds, *Water Research*, 2014, **48**, 210-217.